Parallel optimization of tumor model parameters for fast registration of brain tumor images

Evangelia I. Zacharaki[*a], Cosmina S. Hogea[a], Dinggang Shen[a], George Biros[b], Christos Davatzikos[a]
[a]Section of Biomedical Image Analysis, University of Pennsylvania, Philadelphia PA, USA
[b]Dept. of Mechanical Engineering and Applied Mechanics, University of Pennsylvania Philadelphia PA, USA

ABSTRACT

The motivation of this work is to register MR brain tumor images with a brain atlas. Such a registration method can make possible the pooling of data from different brain tumor patients into a common stereotaxic space, thereby enabling the construction of statistical brain tumor atlases. Moreover, it allows the mapping of neuroanatomical brain atlases into the patient's space, for segmenting brains and thus facilitating surgical or radiotherapy treatment planning. However, the methods developed for registration of normal brain images are not directly applicable to the registration of a normal atlas with a tumor-bearing image, due to substantial dissimilarity and lack of equivalent image content between the two images, as well as severe deformation or shift of anatomical structures around the tumor. Accordingly, a model that can simulate brain tissue death and deformation induced by the tumor is considered to facilitate the registration. Such tumor growth simulation models are usually initialized by placing a small seed in the normal atlas. The shape, size and location of the initial seed are critical for achieving topological equivalence between the atlas and patient's images. In this study, we focus on the automatic estimation of these parameters, pertaining to tumor simulation. In particular, we propose an objective function reflecting feature-based similarity and elastic stretching energy and optimize it with APPSPACK (Asynchronous Parallel Pattern Search), for achieving significant reduction of the computational cost. The results indicate that the registration accuracy is high in areas around the tumor, as well as in the healthy portion of the brain.

Keywords: brain tumor, deformable registration, atlas-based segmentation, tumor simulation, APPSPACK

1. INTRODUCTION

Deformable registration is widely applied in neuroimaging in order to register generally normal neuroanatomies in a common space and apply voxel-based morphometry or automated segmentation methods. Voxel-based morphometry allows the investigation of focal differences in the brains by integrating a variety of patient data of a large number of patients into the same space. Although population-based statistics have been performed in a variety of studies of normal brain development and aging, as well as of brain diseases such as Alzheimer's or mild cognitive impairment [1][2], they haven't been applied in studies of brain cancer. For example, studying the tumor origin and location relative to brain structures for different types of tumors could help gain insight into the brain tumor disease. Moreover, the spatial normalization of tumor diseased images into a common template space, before and after treatment and especially when tumor has recurred, could help studying the tumor progression in relation to the applied treatment.

Besides the potential value of deformable registration of pathological brain images with an atlas for statistical parametric mapping, it is also useful for performing atlas-based segmentation for the neurosurgical treatment planning. Thus, atlases with segmented structures of interest or with integrated information about anatomical and functional variability can be mapped into the patient's image space in order to minimize the risk for significant functional impairment.

The application of registration methods designed to register generally normal neuroanatomies [3] can lead to poor registration when applied to brain images with large tumors, due to large deformations and lack of clear definition of anatomical detail in a patient's images. Specifically, in the images with tumor, the fundamental assumption of topological equivalence between the atlas and the patient's image, which is almost ubiquitous in deformable registration methods, is violated due to the anatomical changes caused by tissue death and tumor emergence. Moreover, the large distortions caused by the mass effect of a growing tumor violate the usual assumption of smoothness of the deformation fields.

*Eva.Zacharaki@uphs.upen.edu; phone 1 215 614-1824; fax 1 215 614-0266; www.rad.upenn.edu/sbia

Medical Imaging 2008: Image Processing, edited by Joseph M. Reinhardt, Josien P. W. Pluim,
Proc. of SPIE Vol. 6914, 69140K, (2008)
1605-7422/08/$18 · doi: 10.1117/12.767788

Most methods that have been proposed to deal with this registration problem first create topologically equivalent images by either removing the tumor from the patient or by placing a small tumor seed in the atlas. Other methods just ignore the regions within and around the tumor with the risk of containing singularities inside those regions. Brief discussion on the most representative methods can be found in [4]. A more analytical survey and classification of those methods according to the type of registration, tumor model and main limitations is presented by Cuadra *et al.* [5]. We agree with the authors in [5] that a model of deformations induced by the tumor is a desirable property for such a registration framework, since it ensures the continuity of the transformation in the tumor area and preserves from any irregularities that could appear in this region due to the lack of equivalent image content between atlas and patient images.

After seeding the atlas, some methods simulate the tumor induced deformation, in order to resolve the geometric discrepancies from the physiologic process of tumor growth prior to registration, whereas other methods adapt locally the elasticity of transformation, in order to allow large deformations around the tumor during registration. In both cases, the patient-specific tumor seeding parameters should be estimated. These parameters can be 3 (location of a single-voxel seed), 4 (if spherical seed), or larger if an arbitrary shape is used. Since these parameters control the amount of topological equivalence between the atlas and patient's image, a larger number of parameters shouldn't be considered as a limitation of the method [5]. It is difficult to determine which number of parameters is the best trade-off between flexibility, computational cost and ability for estimating those parameters (solving the inverse problem). For the methods that simulate the tumor induced deformation, additional parameters are required related to the tumor growth model applied (e.g. material constitutive law). The number of parameters increases, if more advanced biophysical models are integrated that incorporate the effects of peri-tumoral edema and tumor infiltration.

The study presented in this paper is based on the ORBIT framework [4][6] and includes tumor seeding, simulation of tumor growth and calculation of a dense deformation field that maps the (deformed) atlas with simulated tumor to the patient's image. The registration component is based on the assumption that there is equivalent image content between the atlas with simulated tumor and the patient's image, and the deformation between the tumor-bearing images is smooth, similar to normal-to-normal image registration. In this study, (i) we apply a biomechanical model, developed in an Eulerian formulation and solved using regular grids in a fictitious domain method, which is significantly faster than common finite element models and (ii) focus on the automatic estimation of the tumor model parameters pertaining to tumor simulation. In particular, we propose an objective function for assessing the optimality of tumor simulation / registration and optimize it with the parallel optimization method, APPSPACK (Asynchronous Parallel Pattern Search), aiming at significantly reducing the computational cost.

2. METHODS

Fig. 1 illustrates the whole framework for registration of a normal atlas with a tumor-bearing brain image (patient's image), which involves three components: (i) simulation of tumor growth in the atlas image, (ii) deformable registration between the atlas with simulated tumor and the patient's image, and (iii) assessment of the output (i.e. deformation field and registered atlas) for estimation of the tumor model parameters.

Tumor growth is simulated by seeding the atlas. The approach we use to simulate the tumor induced deformation (mass effect) is based on a biomechanical model employing incremental linear elasticity [7]. The atlas with simulated tumor is subsequently registered with the patient's image using a deformable registration method, which is built upon the idea of HAMMER registration algorithm [8] and which follows a deformation strategy that is robust to the confounding factors caused by the presence of tumor [4]. The tumor model parameters are estimated by optimizing a function that reflects feature-based similarity and elastic stretching energy using APPSPACK. The three components of this framework (tumor growth simulation, deformable registration and optimization of model parameters) are described with more details in sections 2.1, 2.2 and 2.3, respectively.

2.1 Tumor growth simulation

Since brain tumor images often exhibit large tumors, the biomechanical simulator needs to be robust to large deformations and also computationally efficient, particularly for registration purposes. In [9] we have evaluated the impact that two biomechanical simulators have on the accuracy of deformable registration. The first simulator [10], used in [1][6], is based on a finite element model of nonlinear elasticity and unstructured meshes using the commercial software package ABAQUS. The main draw-backs of this simulator are that: 1) unstructured meshes deteriorate significantly in the presence of large deformations induced by a growing brain tumor, thus frequent remeshing may be needed [10]; 2) the method is computationally slow, since construction of efficient solvers for the resulting algebraic

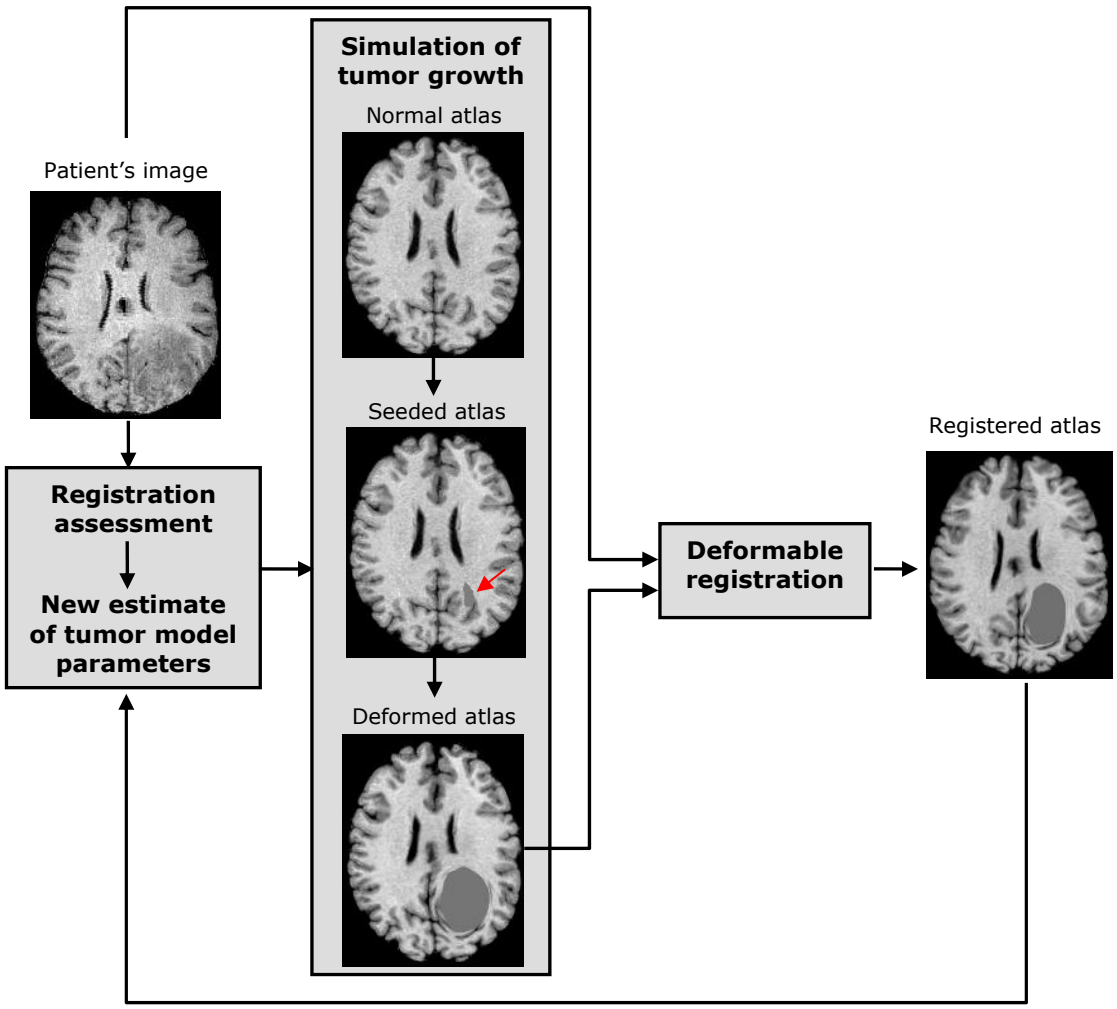

Fig. 1. Illustration of our framework for registration between a normal brain atlas and a patient's image. The red arrow shows the seed that is placed in the atlas for simulating tumor growth. The atlas with simulated tumor (deformed atlas) is then registered to the patient's image.

system of equations is difficult. The second approach [7] was proposed to bypass these inherent difficulties associated with the previous simulator. An incremental pressure, linear elasticity, model was developed in an Eulerian formulation and solved using regular grids in a fictitious domain method. This approach circumvents the need for mesh generation and remeshing. Thus, large deformations can be captured effortlessly and efficient solvers can be employed. The comparison of the two simulators [7][10] on a limited number of subjects showed that the gain in accuracy by using the first simulator was insignificant compared to the additional computational load imposed by it [9]. Therefore in this study we are using the second simulation framework that we shall refer to as *Piecewise Linear Eulerian* (PLE).

More specifically, in the PLE simulator, the brain is approximated as an inhomogeneous isotropic linear elastic medium, with different material properties in the white matter, gray matter and ventricles. In this framework, ventricles are treated as a soft compressible elastic material [7]. For simplicity, zero displacements are imposed at the skull. The target domain (brain) is embedded in a larger computational cubic domain (box), with material properties and distributed forces chosen so that the imposed boundary conditions on the true boundary (here consisting of the brain surface and the tumor boundary, respectively) are approximated. An Eulerian formulation is employed to capture large deformations, with a level-set based approach for evolving fronts. The problem is solved using a regular grid discretization with a fast matrix-free multigrid solver for the resulting algebraic system of equations. The methodology is described in detail in [7].

For the simulations in this paper, we assume that the parameters pertaining to the biomechanical model, such as material properties of brain and ventricles, are similar across patients and we don't include them in the optimization process; we use the same material properties as calculated in [7]. The remaining parameters, that need to be estimated, relate to the patient-specific tumor characteristics. Specifically, the tumor seed is created by eroding the tumor in the patient's image and placing it in the atlas. The size of the eroded tumor and the location in the atlas are the 4 parameters pertaining to the tumor seed. The tumor mass effect is calculated by the act of outward forces normal to the tumor boundary. In order to avoid overlapping forces, the convex hull of the tumor seed is used in the simulations. In order to simplistically distinguish between tumor mass effect (causing brain tissue displacement) and tumor infiltration (not causing displacement) we introduce a 5th parameter, the tumor growth factor. The tumor growth factor is a parameter that allows the simulation of tumor mass effect to terminate before the tumor in the atlas has reached the size of the tumor in the subject. It is introduced to make the registration robust to inaccuracies in tumor segmentation, since for many tumor types it is very difficult to distinguish the boundary between tumor bulk and tumor infiltration/edema.

2.2 Deformable registration of brain tumor images

The elastic deformation field is calculated in a multiresolution scheme according to the hierarchical approximation of an energy function, which consists of the similarity matching criterion defined in the template space, a constraint on the inverse matching, and smoothness constraints on the displacement field, following the general framework of the HAMMER algorithm [8]. The similarity criterion is designed based on the similarity of attribute vectors, which are defined for each voxel in the image in order to capture the anatomical context (including healthy and malignant tissue) around it. Specifically, the attribute vector, $\mathbf{a}(\mathbf{x}) = [\mathrm{a}_1(\mathbf{x}) \quad \mathrm{a}_2(\mathbf{x}) \quad \mathbf{a}_3(\mathbf{x}) \quad \mathrm{a}_4(\mathbf{x}) \quad \mathrm{a}_5(\mathbf{x})]$, reflects edge type ($\mathrm{a}_1$), tissue type ($\mathrm{a}_2$), and geometric moment invariants ($\mathbf{a}_3 = \{\mathrm{a}_3^{(j)}, j = 1,..,K\}$) from all tissue types, respectively. a_1 and a_2 are scalars taking discrete labels, whereas $\mathbf{a}_3$ is a $1 \times K$ vector comprising the geometric moment invariants of each tissue and is used to capture shape information, as described more analytically in [8]. In this application, only zero-order regular moments are used. The number of tissue types depends on the segmentation method applied to labeling brain tissue. Besides the attributes that capture brain structure information, the attribute vector captures also the geometric location relative to the brain tumor. Specifically, a_4 is used to reflect the signed distance from the tumor boundary, and a_5 to reflect the angular location with respect to the tumor center.

The elastic deformation field that spatially warps the template to the patient's image is calculated by maximizing a similarity criterion reflecting the distance of attributes. Specifically, the similarity of two voxels $\mathbf{x}$ and $\mathbf{y}$ is defined as the weighted summation of a similarity criterion matching the brain structures, Sim_B, and a similarity criterion matching the tumor geometry, Sim_T, as given below:

$$Sim(\mathbf{x},\mathbf{y}) = (1 - w(\mathbf{x},\mathbf{y})) \cdot Sim_B(\mathbf{x},\mathbf{y}) + w(\mathbf{x},\mathbf{y}) \cdot Sim_T(\mathbf{x},\mathbf{y}) \tag{1}$$

where

$$Sim_B(\mathbf{x},\mathbf{y}) = \begin{cases} 0, & if\ \mathrm{a}_1(\mathbf{x}) \neq \mathrm{a}_1(\mathbf{y}) \\ \left(1 - \left|\mathrm{a}_2(\mathbf{x}) - \mathrm{a}_2(\mathbf{y})\right|\right) \cdot \prod_{j=1}^{K} \left(1 - \left|\mathrm{a}_3^{(j)}(\mathbf{x}) - \mathrm{a}_3^{(j)}(\mathbf{y})\right|\right), & otherwise \end{cases}$$

$$Sim_T(\mathbf{x},\mathbf{y}) = \exp\left(-c_1 \cdot \left|\mathrm{a}_4(\mathbf{x}) - \mathrm{a}_4(\mathbf{y})\right|\right) \cdot \exp\left(-c_2 \cdot \left|\mathrm{a}_5(\mathbf{x}) - \mathrm{a}_5(\mathbf{y})\right|\right)$$

$$w(\mathbf{x},\mathbf{y}) = \begin{cases} 1, & \mathbf{x}\ or\ \mathbf{y}\ inside\ the\ tumor \\ \dfrac{c_3}{\mathrm{a}_4(\mathbf{x}) \cdot \mathrm{a}_4(\mathbf{y})}, & otherwise \end{cases}$$

$w(\mathbf{x},\mathbf{y})$ is a weighting factor which decreases with the distance of $\mathbf{x}$ and $\mathbf{y}$ from each tumor respectively, and c_i are positive constants. If at least one of the two images is normal (without tumor), the distance from tumor boundary (a_4) becomes infinite, w becomes zero (for the region outside the tumor) and the similarity criterion matches only the brain structures. The use of spatially adapted weights ensures that the identification of corresponding points is driven mainly by one of the two matching criteria, whereas the spatially smooth decrease of w makes the total similarity, *Sim*, smooth. Regarding the intrinsic difference between the similarity criteria, we should note that the function values of both Sim_T and Sim_B are normalized in the range [0, 1]. Moreover, the constants c_1 and c_2 determine the sensitivity (gradient) of Sim_T.

Details on the deformation mechanism, and the mechanism for improving the robustness of the method to slightly inaccurate estimates of the tumor simulation parameters or to unreliable matches caused by the presence of tumor can be found in [4].

2.3 Estimation of the tumor model parameters

We estimate the tumor model parameters by solving a bound-constrained nonlinear optimization problem:

$$\begin{aligned} &\min f(\boldsymbol{\theta}) \\ &s.t.\ L \le \boldsymbol{\theta} \le U \end{aligned} \tag{2}$$

where $f : \Re^n \to \Re$ is an empirical nonlinear function designed to rate the success of the coupled tumor simulation and inter-subject registration problem, $\boldsymbol{\theta} \in \Re^n$ represents the parameters of the tumor simulation model applied, and L and U are lower and upper bounds on $\boldsymbol{\theta}$, respectively. In this application, we focus only on the model parameters that are patient-specific, such as the origin of the tumor (3D Cartesian coordinates), the amount of brain tissue that died due to the tumor appearance, and the tumor growth factor. The bounds L and U are putting some constraints on the validity of the simulations. For example, the search for the optimal tumor center is bounded within 12*mm* from the initial estimate. Non-linear constraints describing the complex brain domain - which excludes the ventricles - are not explicitly handled; instead, a penalty function is imposed to inhibit invalid tumor simulations (e.g., outside the brain). An upper bound on the tumor growth factor (amount of expansion) is the size of the tumor in the subject's image.

2.3.1 Objective function

The objective function used for optimizing the tumor model parameters is based on the hypothesis that the optimal tumor parameters minimize the discrepancies between the co-registered images and also produce realistic deformation maps when trying to match the atlas with simulated tumor with the patient's image. The objective function, *f*, reflects the success of registration and the validity of the calculated deformation fields and is expressed as feature-based similarity and elastic stretching energy, respectively. Specifically, it is defined as the combination of three normalized measures: (i) the overlap of the co-registered segmented images (E_1), (ii) the feature-based similarity as in equation (1) (E_2)[4], and (iii) the Laplacian of the inter-subject deformation field which is used to rate the regularity of the solution based on smoothness properties (E_3), as mathematically given below.

$$f = \sum_{k=1}^{3} \sum_{\mathbf{x} \in \Omega} c_k h_k(\mathbf{x}) E_k(\mathbf{x}; \boldsymbol{\theta}) \tag{3}$$

The constants c_k are used to assign different weights on different measures, whereas $h_k(\mathbf{x})$ is used to assign different weights according to the voxel's location $\mathbf{x}$. $h_k(\mathbf{x})$ is selected to decrease with the distance from the tumor boundary for all three measures, and to increase on voxels lying on edges particularly for the image-related measures, i.e., E_1 and E_2. The assignment of higher weights on voxels lying on edges is due to the distinctiveness of the features of those voxels. The constants c_k are learned by evaluating the performance of each measure separately in the registration of patient images, i.e., how informative each measure is in estimating $\boldsymbol{\theta}$. Ω is the domain over which *f* is calculated, and it is defined in the subject brain within a specific distance from tumor boundary, where the effects of mis-registration are expected to be more prominent. The part of the image that has no tissue label due to low confidence in tissue segmentation (e.g. peri-tumorous edema), is excluded from Ω.

2.3.2 Optimization method and strategy applied

The first task is to remove skull from the brain [11] and segment the atlas and individual MR images into white matter (WM), gray matter (GM) and cerebrospinal fluid (CSF) using FAST (FMRIB's Automated Segmentation Tool) [12]. After tissue segmentation, different labels are assigned to ventricular CSF and cortical CSF by using a modified version of HAMMER. The tumor is manually delineated by an expert in the patient's original image. Subsequently, the patient's image is registered globally with the tumor-free template (indicated as *normal atlas* A_0 in Fig. 2) by applying an affine transformation [13]. The transformed image is denoted as *affine transformed subject* in Fig. 2.

Then the tumor parameters $\boldsymbol{\theta}$ are optimized by solving equation (2). We chose a derivative-free method to obtain a solution to equation (2), because the objective function contains discontinuities and the approximations of the derivatives with finite differencing may be unreliable. Pattern search methods are considered to be effective for solving such

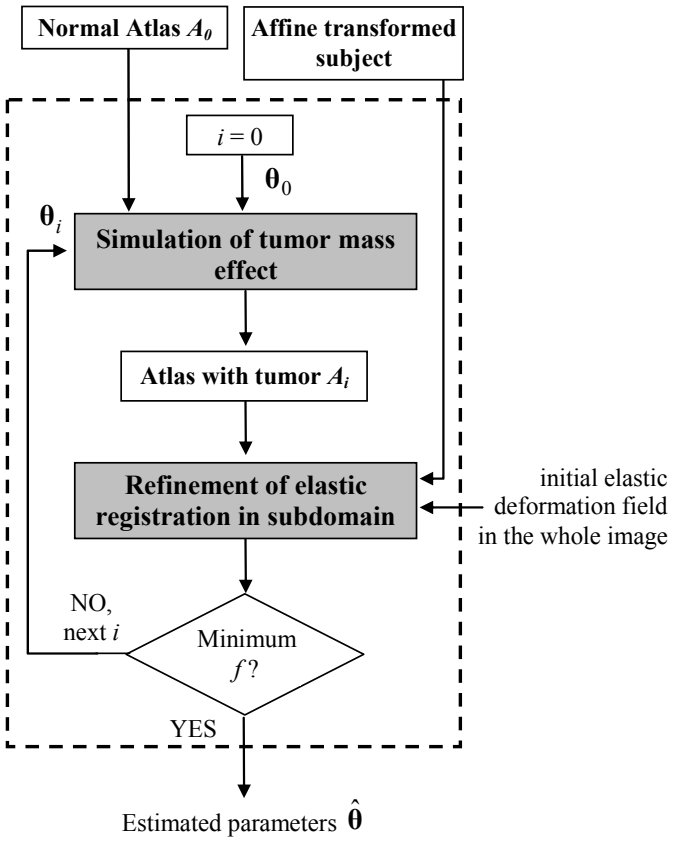

Fig. 2. Estimation of the tumor model parameters by evaluating and maximizing $\boldsymbol{f}$ in a subdomain of the subject space (region around the tumor).

problems. Since the majority of the computational cost is the function evaluation, we apply an Asynchronous Parallel Pattern Search method, called APPSPACK [14], which takes advantage of parallel platforms. APPSPACK targets simulation-based optimization problems characterized by a small number of parameters. The "asynchronous" property is important for our application, since the function evaluation cost varies significantly according to the parameters applied.

The tumor model parameters, $\boldsymbol{\theta}$, are optimized in a coarse to fine resolution scheme. For each resolution level, an initial estimate of the deformation field is obtained by elastically registering the *affine transformed subject* to the *normal atlas* in the whole image domain. Since the deformation field displays almost negligible changes in the regions far away from the tumor during the iterative process of optimizing $\boldsymbol{\theta}$, the optimization is performed only in a subdomain of the subject space in order to considerably speed up the implementation. The subdomain is larger than the tumor neighborhood, Ω, used to evaluate the optimality criterion.

3. RESULTS

We have applied the proposed framework for registration of 16 brain MRI datasets including tumors of different types, grade and sizes. All images are registered with a normal brain image serving as a template, with the image size of 256×256×198 and the voxel size of 1×1×1 mm^3.

One registration example of a diffuse and infiltrative tumor is shown in Fig.1 as part of the illustration of the proposed framework. Fig. 3 illustrates other results obtained by warping the normal atlas (shown on the first row) onto three brain images with tumor. Three labeled regions on the atlas, i.e., thalamus, caudate nuclei, and ventricles (shown with lila, green and pink, respectively), are mapped after registration onto the patient's images, in order to visualize the registration performance on anatomical structures deformed by the tumor.

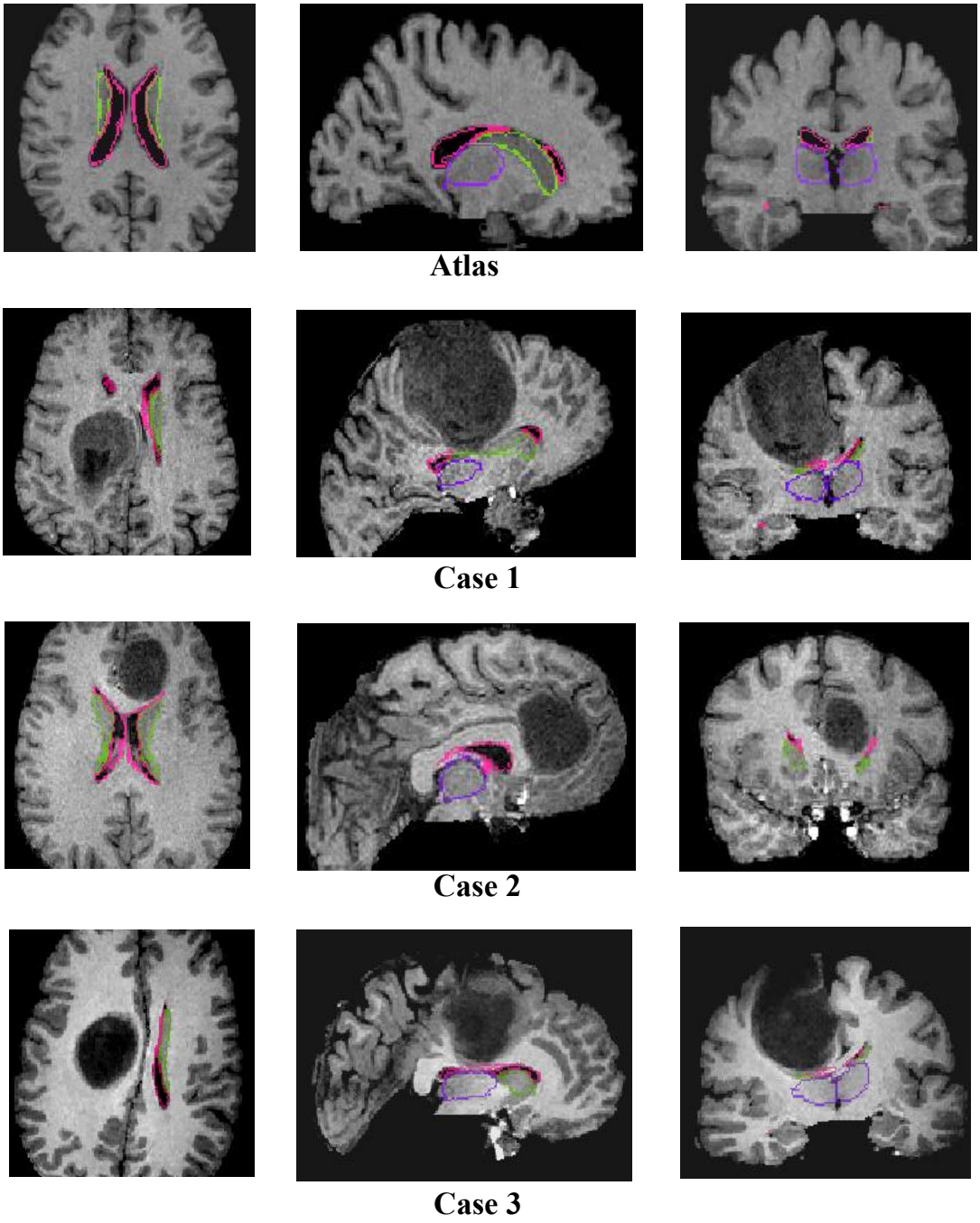

Fig. 3. Application of the proposed method to atlas-based segmentation of brain tumor images. Contours of the thalamus, caudate nuclei, and ventricles, shown with lila, green, and pink, respectively, are registered and superimposed from the normal atlas to three patient's images.

Besides providing the qualitative results based on visual assessment, we calculated a quatitative rater-independent measure, such as the surface distance of the ventricles (*VN-dist*) between the co-registered images. We calculated *VN-dist* as the mean Euclidean distance of the ventricular boundaries in both directions, from the patient's image to the warped atlas image and reversely. We selected the ventricles for validation, because they are structures with distinct boundaries providing accurate (automatic) segmentation. Table 1 shows *VN-dist* for 16 patient's images calculated over

Table 1. VN-dist (in *mm*) for 16 patient's images.

Total boundary	No. 1-8	1.394	0.998	1.118	0.986	0.872	**2.758**	0.785	0.997
	No. 9-16	0.752	1.021	1.254	1.050	1.000	0.8970	1.010	1.895
In tumor vicinity	No. 1-8	1.578	1.098	1.165	1.349	1.099	**3.662**	0.578	1.430
	No. 9-16	0.657	2.350	1.436	1.039	1.479	2.076	2.745	1.860

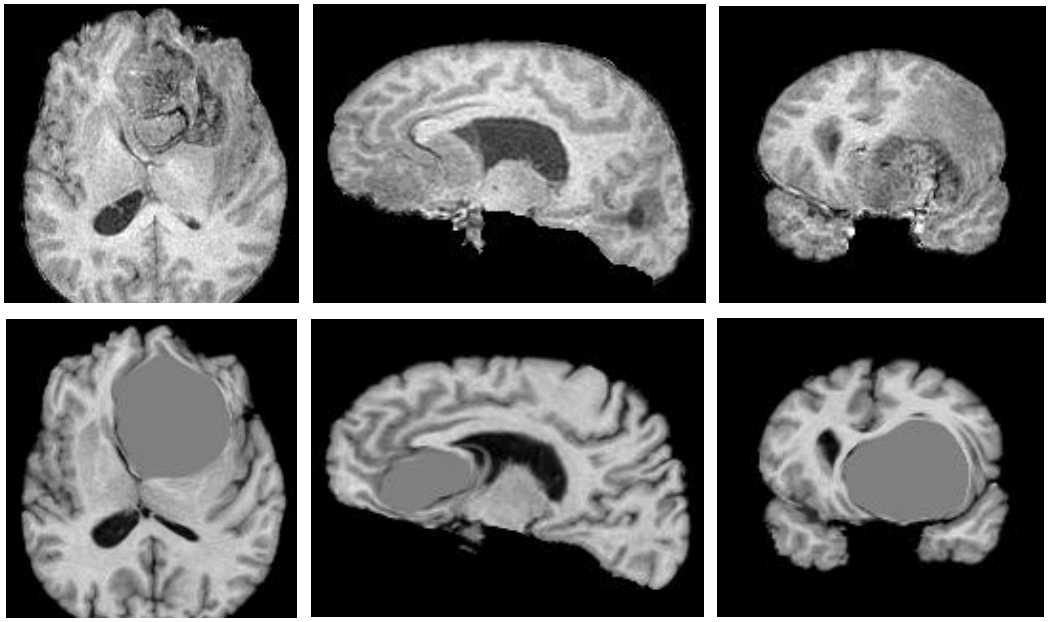

Fig. 4. Registration of a normal atlas image to the patients' images with the highest error (*VN-dist* = 2.758 *mm***)**. The first row illustrates a section of the skull stripped T1-weighted patient's image (axial, sagittal, or coronal). It can be seen that the anatomy is highly obscured by tumor infiltration and edema. The second row shows the corresponding section of the atlas warped with the proposed framework.

the whole ventricular boundary (top rows), as well as only on the part that lies closer to the tumor, in order to emphasize possible limitations of the method due to the presence of tumor (bottom rows).

These results show that the distance of ventricles is larger in the tumor vicinity than over the total ventricular boundary. Specifically, the error is at voxel accuracy for the ventricular part that is far from the tumor and at the order of the diagonal voxel distance for the region close to the tumor, for all cases except for one. This worst case, which is highlighted in Table 1, has an error of 2.758 *mm* and 3.662*mm* respectively and is shown in Fig.4. It can be seen that this is a very difficult case, from image registration perspective, since the anatomy is highly obscured by tumor infiltration and edema, and the ventricles cannot be clearly segmented.

In the future we plan to test our proposed method on more data and use expert defined ground truth, for more extensively assessing registration accuracy.

4. DISCUSSION AND CONCLUSIONS

Although a large number of algorithmic approaches exist for registration of normal brain images, the methods proposed for registering brain tumor images in a stereotactic space, i.e. with a tumor free template, are quite limited. In this study we present a method for brain atlas registration in the presence of tumors which is based on the idea of decoupling the total deformation into the tumor induced deformation and the deformation due to inter-subject differences, similarly as in [4][6] and [15]. The current framework differs in the following components from previous studies in our group:

(i) *Tumor simulation*: The current framework uses a piecewise linear elasticity model and regular grids (PLE

simulator), versus a finite element model of nonlinear elasticity and unstructured meshes in [6][15] and a local-PCA based model in [4]. The PCA-based model was introduced in [4] to considerably reduce the computational cost during optimization, since the PLE simulator was not yet available. Due to the approximate nature of PCA-based models (the solution is approximated based on precalculations during training), here we prefer using efficient biomechanical simulators, such as the PLE.

(ii) *Optimization of the tumor model parameters*: It applies the APPSPACK optimization package for parallel optimization (using mpi) of 5 tumor-related parameters, versus the *Downhill Simplex* method in [4] for serial optimization of 4 parameters, and a statistical approach in [15], not based on optimization, applied for a different sets of parameters (edema was also defined in [15]).

(iii) *Definition of the tumor model parameters*: It applies irregular shaped convex seeds, versus spherical seeds in [15] and irregular seeds without convexity constraint in [4]. The use of irregular seeds allows the creation of an atlas with tumor that is more similar to the subject's image.

(iv) *Registration method*: It is based on a deformation strategy that is robust to unreliable matches caused by the presence of tumor, as in [4], versus the regular HAMMER registration algorithm developed for normal brains in [15].

Our results, based on visual assessment, indicate that the proposed method performs well in both areas around the tumor and in the healthy portion of the brain. More importantly, the computational time is considerably decreased in comparison to our previous work [4], due to the use of parallel optimization for the parameters of the tumor growth model. Due to the different tumor modeling approaches used here and in the original ORBIT framework [4], we cannot compare the computational cost. The computational cost increases with the number of resolution levels applied in the optimization of the tumor model parameters and decreases with the number of parallel processors. The current results have been produced by optimizing the tumor model parameters only in the middle resolution level and using 20 parallel processors. The execution time for optimizing the parameters in the subdomain ranged from 1.1h to 4h depending on the load of the processors, the closeness of the initial estimate to the optimum and the size of the tumor (the tumor growth simulation takes longer for larger tumors). The whole framework (starting from the segmented atlas and patient's images), which includes the steps implemented serially in a single processor, required about 2 hours additionally to the optimization. These steps are the calculation of the global alignment, the calculation of the deformation field in the whole image domain before the estimation of $\boldsymbol{\theta}$ (for initialization) and the calculation of the deformation field in the whole image domain after the estimation of $\boldsymbol{\theta}$ (for refinement in the full resolution).

The tumor model parameters are critical for achieving topological equivalence between the atlas and patient's image, and any assumptions on those limit the possible simulation outcomes. However, we believe that the estimation of the tumor parameters is more important in the case of spatially normalizing brain tumor images into a common (atlas) space, than in the case of atlas-based segmentation (when a normal atlas is mapped into the patient's image space). Small variations in the tumor seed have small effect in the registration of the atlas to the subject space, although the image differences are prominent in the original, undeformed atlas space. Therefore, methods that have been originally developed with the purpose of atlas-based segmentation often apply simplistic models of tumor growth (e.g. radial expansion) [16], ignore the information contained within the lesion [17], or do not perform any algorithmic adjustments due to the presence of lesions [18]. On the other hand, for the purpose of performing population-based statistics, the flexibility of the tumor growth simulation and the ability of estimating the model parameters describing the tumor development, becomes essential. Although the parameters estimation requires additional computational cost, we believe that the better understanding of the tumor development, such as knowledge of the origin of the tumor or the amount of tissue death, is of high clinical importance.

A current limitation of our approach is that it is based on the prior tissue segmentation, which poses considerable difficulties in practice, especially in the region around the tumor that often displays edema and infiltration. The proposed framework is mostly suitable for tumors with distinct tumor boundaries, which are not very challenging from segmentation perspective. However, it is important to note that the current implementation is robust to inaccuracies in tumor segmentation because the simulated tumor is not forced to expand until it reaches the manually segmented tumor in the patient's image. The amount of tumor expansion is rather determined by optimizing the defined optimality criterion. One future extension of the proposed registration method could be the transition from hard tissue segmentation into a fuzzy or probabilistic segmentation framework, which is more appropriate for the inherently diffuse and infiltrative brain tumors cases, since in those cases the tumorous area can only be characterized through probabilistic tissue abnormality maps. On-going work in our laboratory investigates pattern classification methods that use multi-acquisition imaging profiles, including T1, T1-GAD-enhanced, FLAIR, DTI, and aims to achieve a more accurate tissue classification, thereby assisting in the registration process.

REFERENCES

[1] P. M. Thompson, et al., "Cortical Change in Alzheimer's Disease Detected with a Disease-specific Population-based Brain Atlas," *Cerebral Cortex,* 11, 1-16 (2001).

[2] J. Ashburner, J. G. Csernansky, C. Davatzikos, N. C. Fox, G. B. Frisoni, and P. M. Thompson, "Computer-assisted imaging to assess brain structure in healthy and diseased brains," *The Lancet (Neurology),* 2, 79-88 (2003).

[3] J. P. W. Pluim, J. B. A. Maintz, and M. A. Viergever, "Mutual-information-based registration of medical images: a survey," *IEEE Transactions on Medical Imaging,* 22, 986-1004 (2003).

[4] E. I. Zacharaki, D. Shen, S.-K. Lee, and C. Davatzikos, "ORBIT: A Multiresolution Framework for Deformable Registration of Brain Tumor Images," *IEEE Trans. Medical Imaging*, in press (2008).

[5] M. Bach Cuadra, M. De Craene, V. Duay, B. Macq, C. Pollo, J.-Ph. Thiran, "Dense deformation field estimation for atlas-based segmentation of pathological MR brain images," *Computer Methods and Programs in Biomedicine*, 84, 66–75 (2006).

[6] E.I. Zacharaki, D. Shen, A. Mohamed, C. Davatzikos, "Registration of brain images with tumors: Towards the construction of statistical atlases for therapy planning," *3rd IEEE International Symposium on Biomedical Imaging (ISBI 2006)*, 197-200 (2006).

[7] C. S. Hogea, G. Biros, F. Abraham, and C. Davatzikos, "A robust framework for soft tissue simulations with application to modeling brain tumor mass effect in 3D MR images," *Phys. Med. Biol.*, 52, 6893-6908 (2007).

[8] D. Shen, and C. Davatzikos, "HAMMER: Hierarchical attribute matching mechanism for elastic registration," I*EEE Trans. Medical Imaging*, 21, 1421-1439, (2002).

[9] E.I. Zacharaki, C.S. Hogea, G. Biros, and C. Davatzikos, "A comparative study of biomechanical simulators in deformable registration of brain tumor images," *IEEE Trans. Biomedical Engineering*, 55(3), (2008).

[10] A. Mohamed, and C. Davatzikos, "Finite Element Modeling of Brain Tumor Mass-Effect from 3D Medical Images," in *MICCAI*, Palm Springs, CA, pp. 400-408 (2005).

[11] S. M. Smith, "Fast robust automated brain extraction," *Human Brain Mapping,* 17, 143-155 (2002).

[12] Y. Zhang, M. Brady, and S. Smith, "Segmentation of brain MR images through a hidden Markov random field model and the expectation maximization algorithm," *IEEE Trans. Medical Imaging,* 20, 45-57 (2001).

[13] M. Jenkinson, P. R. Bannister, J. M. Brady, and S. M. Smith, "Improved optimisation for the robust and accurate linear registration and motion correction of brain images," *Neuroimage,* 17, 825-841 (2002).

[14] A. Gray and T. G. Kolda, "Algorithm 8xx: APPSPACK 4.0: Asynchronous Parallel Pattern Search for Derivative-Free Optimization," *ACM Transactions on Mathematical Software*, 32(3), 485-507 (2006).

[15] A. Mohamed, E. I. Zacharaki, D. Shen, and C. Davatzikos, "Deformable registration of brain tumor images via a statistical model of tumor-induced deformation," *Medical Image Analysis*, 10, 752-763 (2006).

[16] C. Polio, M. Bach Cuadra, O. Cuisenaire, J.-G. Villemure, J.-Ph. Thiran, "Segmentation of brain structures in presence of a space-occupying lesion," *Neuroimage*, 24(4), 990–996 (2005).

[17] R. Stefanescu, et al., "Non-rigid atlas to subject registration with pathologies for conformal brain radiotherapy," in *MICCAI*, Saint-Malo, France, September 26–29, pp. 704–711 (2004).

[18] P.Y. Bondiau, et al., "Atlas-based automatic segmentation of MR images: Validation study on the brainstem in radiotherapy context," *Int. J. Radiat. Oncol. Biol. Phys*., 61(1), 289–298 (2005).